Facile synthesis and photocatalytic activity of $Bi_2O_3/BiVO_4$ nanocomposites

J. JIANG, X. LUAN, M. CHEN, Q. YANG, L. LI*, M. ZHANG*

School of Chemistry and Materials Science, Huaibei Normal University, Huaibei 235000, China

Using NH_4VO_3 and $Bi(NO_3)_3·5H_2O$ as raw materials, the $Bi_2O_3/BiVO_4$ nanocomposites were synthesized by a simple two-steps process involving ball milling solid-state reaction and subsequent thermal treatment. X-ray powder diffraction (XRD) and UV–Vis diffuse reflectance spectroscopy were employed to study the phase structures and optical properties of the synthesized products. The influences of the experimental parameters such as milling time, annealing time on the phase formation and crystal structure of the synthesized products were studied. At the same time, the photocatalytic experimental results showed that the as-synthesized $Bi_2O_3/BiVO_4$ had a higher photocatalytic efficiency than pure Bi_2O_3 and $BiVO_4$ for the photocatalytic degradation of methyl orange (MO) under visible light irradiation. In addition, the influences of Bi_2O_3 content on the photocatalytic activity of $xBi_2O_3/BiVO_4$ was observed, and 0.3 $Bi_2O_3/BiVO_4$ showed the best photocatalytic activity.

(Received February 9, 2015; accepted March 19, 2015)

Keywords: $Bi_2O_3/BiVO_4$, Composites, Photocatalytic degradation, Solid-state reaction

1. Introduction

Semiconductor photocatalysts have been the focus of considerable attention over the last decades owing to their potential application in environmental remediation and solar energy conversion. Titanium dioxide (TiO_2) is undoubtedly the most popular and widely used photocatalyst for its low cost, high photocatalytic activity, chemical and photochemical stability, and biocompatibility. However, it is only active under ultraviolet light irradiation due to its wide bandgap (ca. 3.2 eV), not responding to visible light ($\lambda > 400$ nm), which is the main component in solar light and indoor irradiations. For this reason, TiO_2 is limited for large-scale industrial applications and indoor use because of insufficient supply of UV light. Hence, a lot of work has been done to develop efficient visible-light-sensitive photocatalysts [1-6].

As is known to all, $BiVO_4$ is a typical n-type narrow band-gap semiconductor, and it has been considered as an excellent visible-light-responsive photocatalyst for the applications in hydrogen production and photocatalytic degradation of organic pollutants under visible light irradiation [7-9]. On the other hand, Bi_2O_3 is a p-type semiconductor, which has been found to possess a narrow band gap because of the hybridized O 2p and Bi 6s valence bands [10]. So it is easy to have a simulated sunlight responsive ability when Bi_2O_3 with special crystal phase is applied as a photocatalyst [11–16]. Unfortunately, the photocatalytic efficiency of single semiconductor is still not high enough for photocatalytic application due to the fast recombination of photoexcited electrons and holes [17]. Thus, novel photocatalysts based on pure $BiVO_4$ or Bi_2O_3 are required to be further explored for practical applications. To improve the photocatalytic efficiency of both $BiVO_4$ and Bi_2O_3, the combination of the two semiconductors may be a good way. The reason is that $BiVO_4$ has suitable band edges (E_{CB}= 0.38 eV, E_{VB}= 2.68 eV), which match well with Bi_2O_3 (E_{CB}=0.33 eV, E_{VB}=3.13 eV) to form a p-n heterojunction, leading to the great improvement of the separation efficiency for photogenerated electrons and holes [18]. So, the improvement of the photocatalytic efficiency may be achieved for $Bi_2O_3/BiVO_4$ according to the principles of semiconductor photocatalysis.

So far, there are a few reports about $BiVO_4$ combination modification with Bi_2O_3 for the improvement of photocatalytic efficiency. Recently, Li et al. [19] reported that $Bi_2O_3/BiVO_4$ submicrometer spheres prepared by the direct physical mixture of Bi_2O_3 and $BiVO_4$ could show much higher photocatalytic activities than pure Bi_2O_3 and $BiVO_4$. However, by a physical mixture method, it is difficult to form an efficient and sound heterojunction, which is crucial to improve the photocatalytic efficiency of the composite photocatalysts. In this paper, $Bi_2O_3/BiVO_4$ composite photocatalyst was synthesized by a facile route combining solid-state reaction with heat treatment process, and p-n heterojunction of $Bi_2O_3/BiVO_4$ was formed in situ solid-state chemical reaction. In the synthesis process, no

solvents, additives, oxidizing and reducing agents are introduced in the system. Here, we develop a more tractable route to synthetize $Bi_2O_3/BiVO_4$ composite photocatalyst with an efficient heterojunction.

2. Experimental

All chemicals used in the study were of analytical reagent grade and used as received. In a typical synthesis process, the initial reactants were firstly mixed together with the different molar ratios of $NH_4VO_3/Bi(NO_3)_3{\cdot}5H_2O$. Then, the mixture was allowed to have a ball milling reaction using the planetary ball mill (QM-3SP04) at the rotation speed of 480 rpm for a certain time at room temperature to obtain the ball-milled precursor. Subsequently, the obtained precursor was washed with water and calcined at 550℃ for 4 hours to get $Bi_2O_3/BiVO_4$ composite with different molar ratios of Bi_2O_3 and $BiVO_4$, which was denoted as $xBi_2O_3/BiVO_4$, where x, from 0.05 to 0.4, was used to describe the molar ratio of Bi_2O_3 and $BiVO_4$.

The ball-milled precursors and the synthesized $Bi_2O_3/BiVO_4$ products were characterized by X-ray powder diffraction analysis, which was carried out on a Bruker D8 Advance X-ray diffractometer equipped with graphite monochromatized Cu Kα radiation (λ= 0.15406 nm) at 40 kV and 40 mA over the 2θ degrees ranging from 10° to 80°. The UV-Vis diffuse reflectance spectra of the synthesized Bi_2O_3, $BiVO_4$ and $Bi_2O_3/BiVO_4$ samples were recorded on a Beijing Purkinje TU-1901 UV–Vis spectrophotometer equipped with an integrating sphere attachment.

The photocatalytic reaction was carried out in a photochemical reactor using a 500 W Xe lamp with a 420-nm UV cutoff filter, and the photocatalytic performance of the synthesized $Bi_2O_3/BiVO_4$ was evaluated by the degradation of methyl orange (MO) in an aqueous suspension under Xe lamp irradiation. The reaction temperature was kept at room temperature by cooling water to prevent any thermal catalytic effect. The reaction suspension was prepared by adding 0.1 g of the photocatalyst powder into 100 ml MO aqueous solutions with the concentration of 20 mg/L. Prior to irradiation, the suspension was magnetically stirred in a dark environment to reach the adsorption/desorption equilibrium between photocatalyst and MO. The degradation of MO was evaluated by centrifuging the retrieved samples and recording the intensity of absorption peak of MO relative to its initial intensity (c/c_0) on a spectrophotometer at its maximum absorption wavelength of 464 nm.

3. Results and discussion

3.1. Synthetic principle of $Bi_2O_3/BiVO_4$ composite

The synthesis of $Bi_2O_3/BiVO_4$ composite photocatalyst is a two-stage process. Firstly, the reactants are ball-milled for a period of time at room temperature, which involves the hydrolysis reaction of $Bi(NO_3)_3{\cdot}5H_2O$ to generate $BiO_{1+x}(NO_3)_{1-2x}$ (where $-1 < x < 0.5$) and the solid state displacement reaction between NH_4VO_3 and $BiO_{1+x}(NO_3)_{1-2x}$ to form the precursor of $BiO_{1+x}(NO_3)_{1-2x}/BiVO_4$. Subsequently, the obtained precursor is heat-treated at 550℃ for a period of time to obtain the $Bi_2O_3/BiVO_4$ product. The formation of the $Bi_2O_3/BiVO_4$ is represented by the following chemical equations:

$$Bi(NO_3)_3 \cdot 5H_2O \xrightarrow{\text{ball milling}} BiO_{1+x}(NO_3)_{1-2x} \quad (1)$$

$$BiO_{1+x}(NO_3)_{1-2x} + NH_4VO_3 \xrightarrow{\text{ball milling}} BiO_{1+x}(NO_3)_{1-2x}/BiVO_4 \quad (2)$$

$$BiO_{1+x}(NO_3)_{1-2x}/BiVO_4 \xrightarrow{calcination} Bi_2O_3/BiVO_4 \quad (3)$$

3.2. Influence of the ball-milling time on phase formation and crystal structure

The XRD patterns of the initial reactants and the precursors synthesized by a ball milling solid-state reaction of NH_4VO_3 and $Bi(NO_3)_3{\cdot}5H_2O$ in a molar ratio of 1:1.6 at different ball-milling times are presented in Fig. 1. It is clearly seen from Fig. 1 that all as-synthesized precursors are composed of the monoclinic $BiVO_4$ phase (JCPDS NO. 14-0688) and the intermediate products. In addition, with the prolongation of the ball milling time, the XRD diffraction peaks of NH_4VO_3 weaken until they disappear after 30 min, indicating that the ball milling time has some influence on the extent of the solid phase chemical reaction, and the reaction of NH_4VO_3 and $Bi(NO_3)_3{\cdot}5H_2O$ is completed within 30 min. The crystallite sizes of $BiVO_4$ calculated from the Scherrer equation are ca. 33.1, 44.3, 36.5 and 32.7 nm corresponding to the ball-milling times of 20, 30, 60 and 90 min, respectively, indicating that the change trend of first increasing and then decreasing in the crystallite sizes of $BiVO_4$ with increasing the ball-milling time during the ball-milling process.

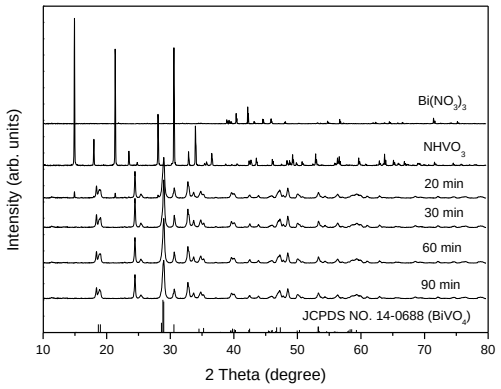

Fig. 1. XRD patterns of initial reactants and the precursors obtained at different ball-milling times.

3.3. Influence of the calcination time on phase formation and crystal structure

Fig. 2 shows the XRD patterns of the $0.3Bi_2O_3/BiVO_4$ products obtained after the milling of 30 min followed by different calcination durations at 550℃ in air. From Fig. 2, all the as-synthesized products are composed of $BiVO_4$ and Bi_2O_3, whose diffraction peaks are indexed to a monoclinic $BiVO_4$ phase (JCPDS NO. 14-0688) and a monoclinic alpha-Bi_2O_3 phase (JCPDS No. 72-0398) respectively, and no characteristic peaks of other impurities are observed. In the as-synthesized products, the mean crystallite sizes of $BiVO_4$ are ca. 65.3、78.1、83.4 and 97.2 nm, and those of Bi_2O_3 are ca. 21.4, 26.1, 31.3 and 38.2 nm, corresponding to the calcination times of 30, 60, 120 and 180 min, respectively, which are calculated from the Scherrer equation. It shows that the mean crystallite sizes of $BiVO_4$ and Bi_2O_3 gradually increase with extending the calcination time, and the mean crystallite sizes of $BiVO_4$ and Bi_2O_3 in the $Bi_2O_3/BiVO_4$ composite can be controlled by varying the calcination time from 30 to 180 min at 550℃.

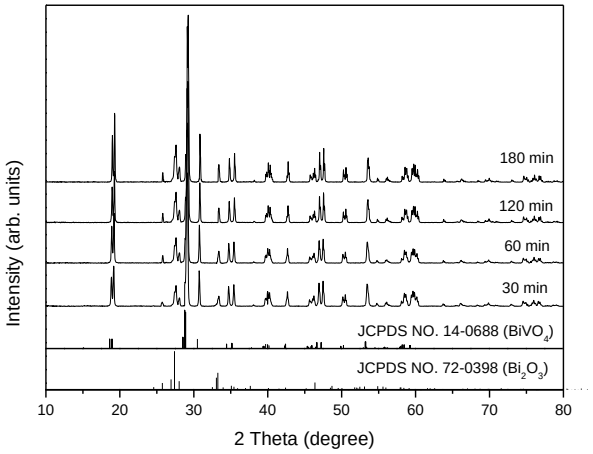

Fig. 2. XRD patterns of the $0.3Bi_2O_3/BiVO_4$ products obtained with the different calcination durations at 550 ℃ in air.

3.4. Optical absorbance spectra and band gap energy

The optical properties of the synthesized products are investigated by UV–Vis diffuse reflectance spectroscopy. Their UV-Vis diffuse reflectance spectra are recorded using $BaSO_4$ as a reference and are converted from reflection to absorbance by the Kubelka-Munk method, and the optical absorbance spectra of $0.3Bi_2O_3/BiVO_4$, $BiVO_4$ and Bi_2O_3 are showed in Fig. 3. As seen from Fig. 3, the absorption onsets of $0.3Bi_2O_3/BiVO_4$, $BiVO_4$ and Bi_2O_3 are 506 nm, 538 nm, 442 nm, respectively. According to the formula $E_g=1240/\lambda_g$, the energy band gaps of $0.3Bi_2O_3/BiVO_4$, $BiVO_4$ and Bi_2O_3 are ca. 2.45 eV, 2.30 eV, 2.80eV, respectively. Moreover, the synthesized $Bi_2O_3/BiVO_4$ composite typically has an intense absorption band with a steep edge in the visible-light region.

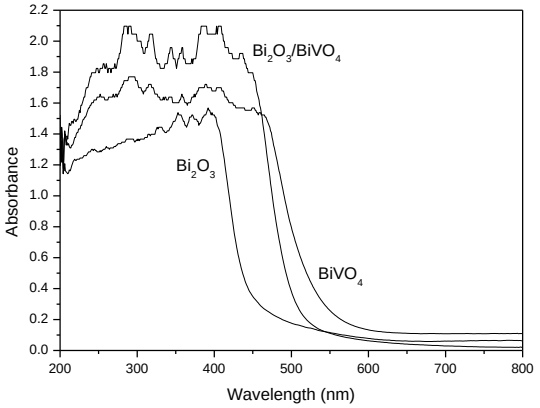

Fig. 3. Optical absorbance spectra of $0.3Bi_2O_3/BiVO_4$, $BiVO_4$ and Bi_2O_3.

3.5. Photocatalytic activities

The photocatalytic activities of Bi_2O_3, $BiVO_4$ and $xBi_2O_3/BiVO_4$ are evaluated through the photodegradation of MO under the visible light irradiation. The experimental results are illustrated in Fig. 4. As a comparison, the photolysis of MO is also carried out in the absence of photocatalyst. It is found that the photodegradation efficiency of MO is negligible in the absence of any photocatalyst. And the $xBi_2O_3/BiVO_4$ composite photocatalysts exhibit much higher photocatalytic efficiency than pure Bi_2O_3 and pure $BiVO_4$. Moreover, the photocatalytic activity of $xBi_2O_3/BiVO_4$ first increase with increasing Bi_2O_3 content and then decrease when the x value is up to 0.4, indicating that there exists an optimal value for the Bi_2O_3 content, namely 0.3:1 of the $Bi_2O_3/BiVO_4$ mole ratio ($0.3Bi_2O_3/BiVO_4$), and the best degradation rate of 84.8 % is achieved over $0.3Bi_2O_3/BiVO_4$ photocatalyst under 500 W Xe lamp irradiation for 180 min.

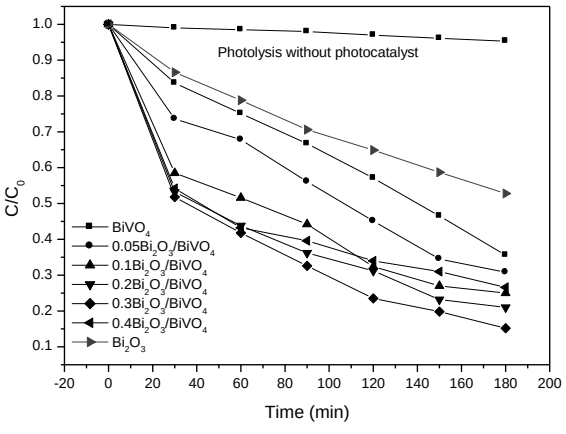

Fig. 4. Photocatalytic activities of $xBi_2O_3/BiVO_4$, $BiVO_4$ and Bi_2O_3.

4. Conclusions

This work provides a facile approach to fabricate visible-light-active $Bi_2O_3/BiVO_4$ nanocomposite photocatalysts, which have been successfully synthesized by a simple solid-state reaction followed by a 550 ^oC thermal treatment. The Bi_2O_3 introduction forms the heterostructured $Bi_2O_3/BiVO_4$ nanocomposite with enhanced photocatalytic efficiency, which can be mainly attributed to the photogenerated electrons and holes separation in the nanocomposite, and the as-synthesized $0.3Bi_2O_3/BiVO_4$ nanocomposite exhibits the highest photocatalytic activity under visible light irradiation. The present study confirms that forming heterostructured nanocomposites is a potentially feasible choice for effective visible-light-active semiconductor photocatalysts.

Acknowledgments

This work is financially supported by Anhui Provincial Natural Science Foundation (No. 1208085MB30), Natural Science Foundation of Anhui Provincial Department of Education (Nos. KJ2013A231, KJ2014A230, and KJ2010A302), and the Earmarked Fund of the State Key Laboratory of Organic Geochemistry (OGL-201213).

References

[1] M. S. Gui, W. D. Zhang, Nanotechnology **22**, 265601(2011).
[2] Y. D. Liu, F. Xin, F. M. Wang, S. X. Luo, X. H. Yin, J Alloy Compd **498**,179 (2010).
[3] J. Mu, Q. L Wei,. P. P. Yao, X. L. Zhao, S. Z. Kang, X. Q. Li, J Alloy Compd **513**,506 (2012).
[4] W. M. Wu, S. J. Liang, L. J. Shen, Z. X. Ding, H. R. Zheng, W. Y. Su, L. Wu, J Alloy Compd **520**, 213 (2012).
[5] M. L. Zhang, C. Feng, W. X. Zhang, X. W. Luan, J. Jiang, L. F. Li, Optoelectron Adv. Mater. **8**, 933 (2014).
[6] L. F. Li, X. W. Luan, C. Feng, J. Jiang, Q. Y. Yang, M. M. Chen, M. L. Zhang, Optoelectron Adv Mater. **8**, 876 (2014).
[7] H. M. Fan, T. F. Jiang, H. Y. Li, D. J. Wang, L. L. Wang, J. L. Zhai, D. Q. He, P. Wang, T. F. Xie, J. Phys Chem C **116**, 2425 (2012).
[8] L. Zhang, D. R. Chen, X. L. Jiao, J Phys Chem B **110**, 2668 (2006).
[9] M. Shang, W. Z. Wang, J. Ren, S. M. Sun, L. Zhang, CrystEngComm **12**, 1754 (2010).
[10] Z. Zhang, W. Wang, M. Shang, W. Yin, J Hazard Mater **177**, 1013 (2010).
[11] R. Chen, Z. R. Shen, H. Wang, H. J. Zhou, Y. P. Liu, D. T. Ding, T. H. Chen, J Alloy Compd **509**, 2588 (2011).
[12] F. Duan, Y. Zheng, L. Liu, M. Q. Chen, Y. Xie, Mater Lett **64**, 1566 (2010).
[13] W. D. He, Q. Wei, X. H. Wu, X. B. Ding, L. Chen, Z. H. Jiang, Thin Solid Films **515**, 5362 (2007).
[14] S. Iyyapushpam, S. T. Nishanthi, D. Pathinettam Padiyan, Mater Lett **86**, 25 (2012).
[15] X. H. Wu, W. Qin, W. D. He, J Mol Catal A-Chem **261**, 167 (2007).
[16] H. Zhang, P. Wu, Y. Li, L. F. Liao, Z. Fang, X. H. Zhong, ChemCatChem **2**, 1115 (2010).
[17] S. Ikeda, N. Sugiyama, B. Pal, G. Marcí, L. Palmisano, H. Noguchi, K. Uosaki, B. Ohtani, Phys Chem Chem Phys **3**, 267 (2001).
[18] L. Chen, S. F. Yin, S. L. Luo, R. Huang, Q. Zhang, T. Hong, P. C. T. Au, Ind Eng Chem Res **51**, 6760 (2012).
[19] L. Z. Li, B. Yan，J Alloy Compd **476**, 624 (2009).

*Corresponding authors: lfli9469@163.com, mlzhang1268@163.com